Published in final edited form as:
J Phys Chem B. 2011 February 10; 115(5): 910–918. doi:10.1021/jp1097519.

Molecular Dynamics and Neutron Scattering Study of Glucose Solutions Confined in MCM-41

Adrien Lerbret[a),#], **Gérald Lelong**[a),b),c)], **Philip E. Mason**[a)], **Marie-Louise Saboungi**[b)], and **John W. Brady**[a),†]

[a)] Department of Food Science, Stocking Hall, Cornell University, Ithaca, NY 14853, USA

[b)] Centre de Recherche sur la Matière Divisée, CNRS – Université d'Orléans, 1b, rue de la Férollerie, 45071 Orléans Cedex 2, France

[c)] Institut de Minéralogie et Physique des Milieux Condensés, Université Paris 6 / CNRS-UMR 7590/Université Paris 7/IPGP/IRD, 140, Rue de Lourmel 75015 Paris, France

Abstract

Glucose aqueous solutions confined in MCM-41 cylindrical pores of diameter 3.2 nm have been studied by molecular dynamics (MD) simulations and quasielastic neutron scattering (QENS). MD simulations reveal a strong preferential interaction of glucose molecules with the silica walls, which induces significant concentration gradients within the pore. The influence of glucose on the structural and dynamical properties of water strongly depends on the region of the pore considered. The distortion of the hydrogen bond network (HBN) and of the tetrahedral organization of interfacial water molecules induced by silica is much stronger than that induced by glucose molecules. The interfacial glucose molecules diffuse about one order of magnitude slower than those in the core region. Differences in affinities for silica of the different species in confined hydrogen-bonded mixtures induce significant structural and dynamical heterogeneities not present in bulk solutions.

Introduction

Eukaryotic cells are extraordinarily complex systems mainly composed of a nucleus and cytoplasm, whose liquid fraction contains a myriad of macromolecules such as proteins, nucleic acids, polysaccharides, etc., all packed into a space delimited by the plasma membrane. The volume occupancy inside the cytoplasm can thus reach 40 % of the total cell volume.[1,2] In this restricted space the inevitable crowding leads to a narrowing of the distances between the different constituents, which can typically reach 1 or 2 nm.[3] In such environments, the major part of the cellular liquid is in immediate contact with the surfaces of the macromolecules, which exert significant influence on the dynamical and structural properties of the liquid.

Such complex systems are difficult to study in their entirety because of the many components and the time/length scales that characterize them. *In vivo* measurements are particularly very hard to interpret in view of the large number of parameters involved: the cellular liquid composition (the presence of salts, ions, sugars, amino acids), the nature of both macromolecules and surface functional groups, the volume of confinement between biological interfaces, etc. It is therefore necessary to break the problem down into simplified

[†]author to whom correspondence should be addressed, jwb7@cornell.edu or mls@cnrs-orleans.fr.
[#]Present Address : Unité Matériaux Et Transformations, UMR CNRS 8207– Université Lille 1, Cité Scientifique, UFR de Physique, Bâtiment P5, 59655 Villeneuve d'Ascq Cedex, France.

schematic models, and more specifically, to study these biological molecules in a confined environment mimicking the length scales of the living world. In recent decades, progresses in organic/inorganic chemistry has allowed the synthesis of porous materials with very well defined mesoporosity and controlled surface chemistry.[4,5,6] Water, which is the canonical biological liquid solvent, was one of the first liquids studied at low dimensionality using porous silica materials as a host matrix (Vycor,[7] SBA-15,[8] MCM-41,[8,9] etc.). Both simulations[10,11,12,13] and experiments[14,15,16,17,18] have shown that the translational diffusion rate is pore size dependent and significantly lowered, by a factor of 2-7 compared to bulk water. The relaxation times are correspondingly increased by several orders of magnitude going from 1 ps to 150 ps in the confined case. These dynamical effects are directly caused by the silica/water interactions via the formation of numerous hydrogen bonds (HBs) with the wall. The first hydration layer is obviously strongly affected by the silica wall, as the decrease of the average coordination number of water shows (N_{bulk} = 3.6 *vs.* N_{conf} = 2.2).[3] Interestingly, the surface, especially in the case of a cylindrical pore, can have an influence on several hydration layers and lead to a layering effect characterized by significant density and residence time oscillations.[12,13,19,20]

Unlike neat liquids, only a few dynamical and structural studies have been reported on binary fluids confined in cylindrical pores in the last years. These include the following mixtures: methanol/water,[21] acetone/water,[22] and isobutyric acid/water.[23] It appears that the hydrophilic/hydrophobic character of each molecule, and their abilities to form HBs with the silanol groups of the wall, can lead to a local demixing at the liquid/solid interface. For example, in the water/acetone mixture, the hydrophobic methyl groups of acetone are localized near the wall,[22] and the same phenomenon seems to occur with methanol molecules in water.[21] It should be noted that very few studies give an overview of the effects of the added molecule (i) on the structure of the HBN of water and (ii) on the dynamical properties of both liquids. In a biological context, it is worthwhile to study the effects of confinement on a model binary solution composed of water and a common solute present in cells, such as glucose, which is the metabolic currency for organisms as well as a powerful bioprotectant agent for cellular membranes.[24]

In this paper, we describe a combined simulation and experimental study of aqueous glucose solutions confined in the mesoscopic pores of a MCM-41 type material.[25,26] In order to depict a general trend of the effects of confinement on a biological binary mixture, a model silica pore that was shown to reproduce satisfactorily structural and dynamical properties of confined water[27] was used here to study the behavior of glucose and water molecules as a function of sugar concentration (0, 0.8 and 2.3 molal) at room temperature. The spatial distribution of sugar and water molecules inside the pore as well as the solute/silica and solvent/silica interactions and their possible effects on the water HBN were explored and quantified. Finally, the translational dynamics of confined glucose molecules determined experimentally by quasielastic neutron scattering (QENS) were compared to calculated values.

1 - Experimental details

1.1 Synthesis – Loading of the solution

Impregnation is the preferred method for loading binary mixtures into mesoporous materials. Several factors are important to insure good filling: (1) a relatively short pore length, (2) a dilute solution to avoid significant concentration gradients along the pore, and (3) a relatively low viscosity of the binary mixture to permit good capillarity. We chose mesoporous silica nanospheres[28] (∅ ≈ 125 nm), which exhibit the shortest pore length (≤ 125 nm) of all existing MCM-41 materials. After a calcination step of 5 hours at 550°C, these mesoporous silica nanospheres exhibited open cylindrical pores with a diameter of 3.2

nm and a surface area of around 700 m^2/g.[28] The host matrix was then outgased in a vacuum oven at 100°C for several hours before being dipped into dilute glucose solutions at 1 and 3 molal (≈ 15 and 35 wt. % in sugar, respectively) for 1-2 hours. The impregnated powder was then filtered, rinsed and finally gently dried in order to extract the water molecules trapped between the spherical particles.

The dynamics of glucose molecules can be revealed in QENS experiments by using hydrogenated sugar molecules in D_2O. However, the situation is complicated by the five exchangeable hydrogen atoms of the glucose molecule. To avoid any exchange between sugar H atoms and the water, the exchangeable protons were deuterated by premixing the sugar with D_2O and drying before dissolving in D_2O.

1.2 QENS experiments

For the QENS experiments, two spectrometers at the National Institute of Standards and Technology - Center for Neutron Research (NCNR) were used: the Disk Chopper Time-of-Flight Spectrometer (DCS)[29] and the High-Flux Backscattering Spectrometer (HFBS).[30] In both cases, the samples were loaded into annular aluminum cans with an annular spacing of 0.4 mm, sealed with indium, and placed within the radiation shield of a closed-cycle refrigerator in which the temperature could be controlled to ± 1 K.

The DCS experiments were carried out at an incident wavelength of 6 Å. The wave vector transfer *Q* (for elastic scattering) covered the range 0.25-1.93 $Å^{-1}$. The sample was measured at 270 and 300 K with run times of approximately 12 h. The energy resolution and intensity normalization were determined from a measurement with a vanadium hollow cylinder under the same conditions as those used for the sample measurements; the resolution was found to be 57 μeV (full width at half maximum (FWHM)), corresponding to a dynamic range of 1-24 ps. The HFBS experiments were carried out at 230K with runs of approximately 30 h using a wavelength of 6.27 Å. The resolution was measured from vanadium to be 1.2 μeV with an energy transfer window of ± 36 μeV, giving a dynamic range of 18 ps-1 ns. The *Q* values covered the range 0.36-1.52 $Å^{-1}$.

The QENS spectra were corrected for container scattering and background, and the scattering functions *S(Q,E)* were obtained, where *E* is the energy transfer. Data sets were reduced and analyzed with the DAVE package.[31]

2 – Computational details

2.1 Pore generation and pore filling procedure

A MCM-41 like mesoporous silica was generated using a procedure described in our previous study of confined water.[27] The cylindrical pore surface was reconstructed in order to reach a final surface silanol concentration of 3 OH/nm^2 in good agreement with experimental data. The pore obtained by this procedure has a diameter of 3.2 nm and was referred to as PL. The last configuration of the water confined in the PL pore has been used as reference sample and two confined solutions with a sugar concentration of 0.8 and 2.3 molal were simulated in this study at room temperature. 21 and 54 sugar molecules, respectively, were superimposed on the final configuration of the confined water simulation.[27] A ratio of one α-anomer for two β-anomers was chosen for glucose to reproduce the anomeric equilibrium.[32] The filling procedure described previously[27] was used to adjust the density of the confined glucose solutions. The total number of confined water was then equal to 1525 and 1290 for the 0.8 and 2.3 m solutions, respectively.

2.2 Confined solution simulation details

All simulations were performed using the CHARMM program[33] in the microcanonical (N,V,E) ensemble, where the number of atoms N, the volume V and the total energy E of the system are constant. The size of the box was 57.0584 Å, and periodic boundary conditions were only applied along the Z direction, corresponding to the pore axis. The lengths of covalent bonds involving H atoms were kept fixed using the SHAKE algorithm[34] and a 1 fs timestep was used to integrate the Newton equations of motions with the Verlet leapfrog algorithm.[35] An atom-based force-switching function[36] was employed to smoothly switch van der Waals forces to zero between 14 and 16 Å, whereas a force-shifting function[37] was used to set electrostatic interactions to 0 at 16 Å. The silica pore atoms were represented with the potential parameter set of Brodka *et al.*[20], which was shown to give satisfying results when coupled with the PL pore.[27] The silica frame was kept rigid by freezing the positions of the O and Si atoms during the simulations. In contrast, rotations of hydrogens around Si-O bonds were allowed: the O-H distance was kept fixed at 0.95 Å using the SHAKE algorithm[34] and the Si-O-H angle was constrained at 116° with a force constant of 5000 kcal $mol^{-1}Å^{-2}$. The CSFF carbohydrate force field[38] was used to simulate glucose molecules, whereas water molecules were represented by the rigid SPC/E model.[39]

The 0.8 and 2.3 m solutions were simulated for 12 ns. Since several nanoseconds were required to reach an equilibrium distribution of glucose molecules inside the pore, the first part of each simulation (8 ns) was considered as the equilibration phase and only the remaining part (4 ns) was considered for the analysis of the equilibrium static and dynamical properties.

3 – Results and discussion

3.1 Simulated structural properties

3.1.1 Water and sugar densities—The organization of water and glucose molecules relative to the pore surface was first qualitatively characterized by their density in the (X,Y) plane, ρ_{XY}, averaged in the Z direction over the pore length (Fig. 1). The intense water density spots close to the pore surface reveal significant localization of water molecules that arises from the strong interaction with the pore and/or the entrapment of water within small surface cavities. Two layers of strongly localized water molecules are clearly observed for pure confined water.[27] The presence of sugars modifies the structuring of water imposed by the solid silica surface. The decrease of the density of interfacial water with increasing sugar concentration is caused by the replacement of water molecules by sugar molecules at the solvent/pore interface. This suggests that sugar molecules are preferentially found in the vicinity of the pore surface, a feature also pointed out by Ziemys and coworkers[40,41] for a different confining geometry (planar silica slabs separated by 10 nm). The positioning of hydroxyl groups around the pyranose rings allows a significant interaction with the curved surface of the silica pore leading to highly localized sugar molecules.

The radial densities $\rho(r)$ of water, glucose and silica are shown in Fig. 2. The density profile of pure confined water clearly exhibits two peaks close to the interface characterizing the layering effect observed in previous simulations on confined monomolecular liquids.[13,19,20,27,42,43,44,56] The addition of glucose induces a decrease in the water density close to the pore surface ascribed to the strong interaction of glucose with the silica pore and characterized by an intense broad peak centered at $r \sim 13$ Å. This leads to a significant decrease of the glucose concentration in the inner part of the pore ($r < 10$ Å), making the confined glucose/water mixture very heterogeneous.

3.1.2 Hydrogen bonds – Glucose preferential interaction—A HB is considered to exist if the O-O distance is less than 3.4 Å and if the O-H---O angle is larger than 120°. Fig. 3 shows the average number of HBs, n_{HBw}, that a water molecule forms with other solution molecules and with the silica matrix. Water molecules with radial positions up to 13 Å form about 4 HBs as in bulk water, but those in the hydration layer of silica can only form 3 HBs. This decrease stems from the significant reduction of the number of water-water HBs at the solvent/pore interface, which is not perfectly balanced by the water-silica HBs, given the rather low silanol surface concentration (3 OH/nm^2) and the rather small dipole of silica hydroxyl groups ($\boldsymbol{\mu}_{OH} \approx 1$ D). The addition of sugar molecules does not change significantly n_{HBw} for the water molecules located in the central part of the mesopore. Moreover, the high concentration of glucose at the interface reduces the n_{HBw} of interfacial water molecules, because the substitution of water-water HBs by water–sugar HBs becomes poorer, so that the water HBN is more distorted (see next section).

The numbers of water-silica and sugar-silica HBs are given in Table 1. The addition of glucose leads to a partial substitution of water-pore HBs by glucose-pore HBs, but in the 2.3 m solution, the total number of solution-pore HBs decreases because of topological constraints that prevent sugars from interacting with the silica pore as extensively as water molecules. The fractions of sugar-pore HBs in the overall solvent-pore HBs (11 and 25% for 0.8 and 2.3 m respectively) are about twice the values calculated on the basis that each water molecule forms 4 HBs and each glucose hydroxyl group 3 HBs. This shows that monosaccharides interact preferentially with the silica surface, in contrast to the generally observed preferential exclusion of sugars from the surface of proteins.[45,46] This opposite behavior can be ascribed to the differences in the polarity and curvature of the corresponding surfaces.[47]

3.1.3 Tetrahedral order parameter—The orientational order parameter *q* quantifies the deviation of the arrangement of water molecules from a perfect tetrahedral network.[48] The *q*-distributions of water molecules in the r ≤ 12 Å region for the solutions studied are shown in Fig. 4a. All distributions have a bimodal shape, similar to that of bulk pure water at ambient temperature. The high-*q* peak may be ascribed to structured (or “ice”-like) water molecules, whereas the low-*q* peak is due to less structured (or “liquid”-like) water. The amplitude of the high-*q* peak decreases while that of the low-*q* peak increases with the addition of sugars (see inset of Fig. 4a). This behavior is similar to that of a slight temperature increase and suggests that glucose distorts the tetrahedral structure of water, in line with the *destructuring effect* of sugars observed in previous studies.[49]

The orientational order parameter averaged over all water molecules $\langle q \rangle$ at a distance *r* from the pore axis is shown in Fig. 4b. The steep decrease of $\langle q \rangle$ for $r > 13$Å probably arises from the location of the O atoms of the pore, which are incompatible with a tetrahedral organization of water molecules. There is a slight additional distortion of the tetrahedral water structure induced by sugars in the interfacial region.

3.2 Dynamics

3.2.1 Neutron Scattering

3.2.1.1 Elastic scans: Energy-resolved elastic neutron scattering scans were performed on HFBS. The elastic intensity is directly proportional to the number of scatterers that are stationary in the time window corresponding to the resolution of the spectrometer (≈ 2 ns). The samples were cooled down to 10 K for 30 min and first heated up to 180K at a rate of 1.4 K/min, and then up to 300K at a rate of 0.2 K/min to allow for full equilibration. Fig. 5 (a) and (b), both normalized by the intensity at $T_{min} = 10$ K, present the temperature scans of the two confined 1 and 3 m glucose solutions and of a bulk 3 m glucose solution. The bulk

solution (Fig. 5 (b)) shows a sharp transition around 275 K related to the melting of the sugar-water solid. The two confined glucose solutions show a smeared transition in the region 200-250 K.

The elastic intensities were fitted by a sigmoid function superimposed on a sloping background:

$$f(T)=A\left(1-\frac{1}{1+e^{-B(T-T_0)}}\right)+(C-DT). \quad (1)$$

The parameters A, T_0, and B represent the amplitude, temperature, and steepness of the transition, respectively. When B tends to zero, the transition can be considered as gradual, and inversely, when B is relatively high, the transition is abrupt. The B parameter can be seen as an indicator of the cooperativity of the system, *i.e.* its ability to crystallize. For clarity reasons, only the fit of the 1 m confined solution is shown in Fig. 5 (a). The fitted values of B are equal to 1.67, 0.11 and 0.14 for the bulk, the 1 m and the 3 m confined solutions, respectively. Clearly, the confinement leads to a significant decrease of the B parameter, indicating a general loss of the cooperativity of the system, i.e., the sugar/water solutions show a tendency for crystallization in the bulk and for vitrification under confinement. Also, the presence of sugar molecules in water leads to a decrease of cooperativity, as shown by the lower B value in the 3 m bulk solution than the value of bulk D_2O (1.8). This observation is fully consistent with the decrease of the melting temperature upon addition of glucose to water and is also supported by the distribution functions of the orientational order parameter q, which show a clear distortion of the water HBN that would hinder crystallization of the glucose solutions at low temperatures. (Fig. 4)

3.2.1.2 QENS Spectra: QENS measurements were carried out on 1 and 3 m confined solutions at temperatures of 230, 270 and 300K. Neither DCS nor HFBS measurements showed a scattering signal in the quasielastic range for the 3 m confined solution. Given the HFBS dynamic range (18 ps-1 ns), this implies that the relaxation times of sugar molecules in such a small environment (≈ 3 nm) are over 1 ns, consistent with the strong localization of glucose molecules at the pore surface observed in Fig. 1.

The dynamical properties of the 1 m confined solution were obtained from an analysis of the scattering function S(Q,E) corrected from the resolution. The best fit was composed of a delta function combined with two Lorentzian functions $L_n(W_n,E)$, where W_n is the full width at half maximum (FWHM) (only one for the HFBS data), and a linear background. The Q dependence of the FWHM of the narrower Lorentzian was least-squares fitted by the following expression used in previous studies on confined solutions,[50,51]

$$W_1=\alpha_1+\frac{\beta_1 Q^2}{1+\gamma_1 Q^2} \quad (2)$$

The fits realized on the DCS measurements at 270 and 300 K are shown in Fig. 6 as continuous and dashed lines, respectively.

The parameters β_1 and γ_1 can be expressed as a function of the translational diffusion constant D and an effective jump distance l,

$$\beta_1 = 2\hbar D \tag{3a}$$

$$\gamma_1 = \frac{l^2}{6}. \tag{3b}$$

Fitted values of *D* and *l* are shown in Table 2 and are compared with our previous study.[50]

It should be noted that the confinement allowed the measurement of glucose diffusion far below the theoretical freezing temperature of a 1 m bulk solution, which is estimated around T_F = 275 K in D_2O.[28] At 300 K, the diffusion coefficient of glucose solutions confined in MCM-41 (3.2 nm) is roughly 30% lower than that obtained for a confinement of 18 nm,[50] which is similar to the value for the bulk solutions. This slowing down is the result of the formation of numerous HBs between solute molecules and the surface silanol groups present inside the mesopore. (Fig. 3 and Table 1) The 30% decrease is comparable to values reported for confined water at room temperature; Takahara *et al.*[15] found a value of 37% (2.8 nm) and Takamuku *et al.*[17] 39% (3 nm). These values indicate that, at the same scale of confinement, sugar and water molecules experience a similar reduction of their translational dynamics, probably caused by similar interactions of both molecules with silica walls. (Fig. 1 and Fig. 2) Below the theoretical freezing temperature, the glucose translational diffusion is slowed down, but 3/5 of the molecular mobility still remains at 270 K and 1/5 at 230 K. At the same time, the jump length distance *l* significantly increases, going from 1.1 Å at 300 K to 4.7 Å at 230 K. This significant increase is indicative of a more chaotic displacement of the sugar molecules when the temperature is reduced. The fit of an Arrhenius relation to the values of the diffusion coefficient gives an activation energy of E_a = 3.2 kcal mol^{-1}, or 13.4 kJ mol^{-1}. The activation energy extrapolated at zero glucose concentration was found to be 4.2 kcal/mol in a previous study.[52] Our results imply that the activation energy for glucose diffusion is lower under nanoscale confinement than in the bulk, as previously observed for confined benzene and glycerol.[53]

3.2.2 Molecular dynamics Simulation

3.2.2.1 Glucose diffusion: The translational diffusion coefficient *D* of molecules can be computed by fitting their mean square displacement (MSD) with the Einstein relation.[27] Given that the cylindrical shape of the pore prevents molecules from diffusing over long distances in the X-Y plane, only the mean-square displacement along the Z axis (MSD_Z) has been considered. The D_Z obtained from the MSD of all molecules reflects an average dynamics of confined molecules. However, several studies showed that the diffusion coefficient of confined molecules strongly depends on the distance from the pore surface.[10,13,40] We therefore computed MSD_Z in different radial regions of the pore, following a procedure described in our previous study on confined water.[27]

The MSDs averaged over all glucose molecules in the two confined glucose solutions are shown in Fig. 7a. Following the ballistic regime (t < 0.5 ps) characterized by a $MSD_Z \sim t^2$, a regime of anomalous diffusion is observed for which $MSD_Z \sim t^{\alpha}$ with $0 < \alpha < 1$. The MSD of glucose molecules is found lower in the 2.3 m solution than in the 0.8 m one, as expected from the dynamical behavior of bulk glucose solutions.[54] The non-linearity of the global MSD of glucose molecules prevents the determination of an accurate diffusion coefficient for this sugar, since the Einstein relation no longer holds for non-Brownian diffusion processes. We therefore decomposed the pore into two regions: a first one where the center of mass of glucose molecules is at r > 10 Å and a second where $r \leq$ 10 Å. The former region

is composed of glucose molecules close to the surface, while glucose molecules in the latter do not interact specifically with the pore and are expected to diffuse similarly to bulk molecules. The MSDs of glucose in these two regions are shown in Fig. 7b-c. The MSD of glucose in the surface region is about an order of magnitude lower than that of glucose in the core region, in good agreement with the results of Ziemys *et al.*, which showed that the glucose diffusivities -computed with a 10 ps window - are reduced by about one order of magnitude at the silica surface compared to the bulk.[40] This significant slowing down is also consistent with the high concentration of glucose in the vicinity of the pore surface (Fig. 1 and Fig. 2) and with the large number of glucose-silica HBs (Table 1). The strong interaction of glucose with the silica as well as the surface rugosity hinders the diffusion of glucose molecules. Furthermore, the larger number of glucose molecules in the 2.3 m solution makes glucose-glucose HBs more likely, and therefore the diffusion of glucose slower. Besides, the MSD of glucose molecules in the core region is nearly linear in the 40-200 ps time interval. This interval has thus been used to compute the approximate diffusion coefficients of glucose in the two solutions, which are reported in Table 3.

Table 3 shows the values of the translational diffusion coefficient along the pore Z axis of the glucose molecules in the core region as well as the bulk diffusion coefficients D extrapolated from those obtained in the simulations of [ref. 54], which employed the same force fields to represent glucose and water molecules. The D_Z/D ratio obtained from simulations is about 1.7 and 1.5 for the 0.8 and 2.3 m solutions, respectively, and suggest that glucose molecules in the inner part of the pores diffuse faster than in bulk solutions. This seems in contrast with the generally observed slowing down of the dynamics of confined solutions in hydrophilic nanopores. However, it can be well accounted for by considering the significant concentration gradient of glucose within the pore. The concentration in the core region was estimated at 0.2 and 0.5 m (*i.e.* 3 and 8 wt.%) for the two confined glucose solutions, respectively. For comparison, Ziemys *et al.*[40] estimated that the local concentration of glucose in the volume where glucoses are not adsorbed onto the silica surface reached 20 wt. %, whereas the average concentration was 26 wt.%. The glucose diffusion coefficient in the simulated 0.8 m solution compares relatively well with the one determined in the QENS experiments at 300 K (Table 2).

3.2.2.2 Water diffusion: The MSD_Z averaged over all water molecules in the different confined solutions are shown in Fig. 8a. The corresponding water diffusion coefficients D_Z are given in Table 4 and are compared to the bulk diffusion coefficients D extrapolated from the simulations of [ref. 54], where the same glucose and water force fields were used. A significant decrease of the global diffusion coefficient of pure confined water is observed (the ratio D_{conf}/D_{bulk} is 0.72) and may arise from the roughness of the pore surface and in particular the presence of small cavities, in which some water molecules are temporarily trapped; and the strong interactions of interfacial water with the silica pore. This slowing down of the water dynamics is in good agreement with results observed in many experimental and simulation studies carried out on pores of different types, sizes and at different temperatures.[55,56] (see [ref. 27]) The addition of glucose leads to an increased slowing down of the water dynamics, also observed experimentally in bulk solutions.[54,57,58] This may be explained by the slower diffusion coefficient of monosaccharide, which sterically hinder water molecules from diffusing as fast as in pure water and interact strongly with water molecules in their close vicinity by forming stable HBs with their hydroxyl groups. However, by comparing the diffusion coefficients extrapolated from [ref. 54] with the present ones, it appears that the slowing down induced by glucose is smaller in the confined solutions. This is ascribed to the large glucose concentration gradients, which make the solution much more heterogeneous than in the bulk.

Since the dynamics of water depends on the distance to the silica walls,[10,13] the MSD of water molecules were computed in three distinct regions of the pore defined radially by $r \leq 9.2$ Å, $9.2 < r \leq 13$ Å, and $r > 13$ Å, and called core, intermediate and surface regions, respectively (Fig. 8b-d). The diffusion of water near the silica surface is strongly subdiffusive, because their motions are hindered by the surface rugosity and because they strongly interact with the silica pore.[27] As a consequence, the diffusion of interfacial water molecules cannot be described by a Brownian process. The MSD of water molecules in the intermediate region is almost linear for pure water, but becomes more sublinear with the addition of glucose. The high density of sugars close to the pore surface makes many water molecules from this region form HBs with glucose molecules (Fig. 3). Finally, the MSD of water molecules in the core region is linear in each solution, and the related D_Z are given in Table 4. For neat water, the diffusion coefficient is in line with those of bulk SPC/E water at room temperature (298-300 K) published earlier (~2.5-2.8 × 10^{-5} cm^2s^{-1})[39,59,60] and agree relatively well the experimental values (2.2-2.3 × 10^{-5} cm^2s^{-1}).[61,62] The diffusion coefficients in the 0.8 and 2.3 m solutions are significantly larger in the core region of the pore than those extrapolated from the corresponding simulations of bulk solutions.[54] This is again well accounted for when considering that the local concentration of glucose in the core region is about 0.2 and 0.5 m, respectively. These results suggest that the effect of glucose on water in our simulations is driven by the strong preferential interaction of glucose for silica. Even though the slowing down on water dynamics clearly appears in the average diffusion coefficient of water, the decomposition of the pore into several radial regions shows that water dynamics is more heterogeneous than one might expect when assuming that water and glucose have similar affinities for the silica walls. Such effects should probably be observed with other confined biological solutions and will have to be taken into account in future biotechnological applications.

Conclusions

The structure and the dynamics of confined aqueous glucose solutions have been investigated by MD simulations and QENS experiments to shed some light on the influence of the confinement experienced by many biological molecules. A model cylindrical pore with a realistic silanol surface density of 3 OH/nm^2, developed in our preceding study,[27] was employed to represent the MCM-41 mesopores used experimentally. A strong layering effect on water induced by the silica pore has been observed. Furthermore, sugars were found to preferentially interact with silica, thereby suggesting strong glucose-pore interactions. The distortion of the water tetrahedral HBN induced by glucose molecules was much weaker than that induced by the silica wall for interfacial water. From a dynamical point of view, elastic scans showed that the confinement leads to a shift of the liquidus line of about 40 K and to deep changes in cooperativity with a tendency for vitrification. The experimental translational diffusion coefficient of glucose in MCM-41 (3.2 nm) was lowered by about 30 % in comparison to that found previously in silica gels (18 nm). The dynamics of glucose in the simulations was spatially very heterogeneous within the pore. The mean square displacement along the pore axis of sugars bound to the silica surface was indeed about one order of magnitude lower than that of glucoses from the core region. These latter sugars even diffused faster than in the corresponding bulk solutions, given the significant depletion of glucose in that part of the pore. The average slowing down of water dynamics induced by confinement is found to be in agreement with previous work, and is amplified by the presence of glucose molecules, although to a lower extent than in the corresponding bulk solutions. As for glucose, the dynamical properties of water were found to be position-dependent, starting from a bulk-like behavior in the core region, at a lower effective glucose concentration, to a subdiffusive regime at the solvent/pore interface.

The present results suggest that the effects of nanoscale confinement on the behavior of hydrogen-bonded binary mixtures not only depend on the topological constraint from the pore, but also on the relative affinities of both molecules for the pore wall that may lead to a local demixing. This effect should be observed in more complex confined biological solutions and will need to be considered in future biotechnological applications.

Acknowledgments

This project was supported by grant GM63018 from the National Institutes of Health in US, the Centre National de la Recherche Scientifique in France, and INSIDE-PORES NoE project (FP6-EU). Helpful discussions and suggestions by Dr. D.L. Price are gratefully acknowledged. We also thank Dr. Felix Fernandez-Alonso, and Drs V. Garcia-Sakai and C. Brown from the NIST Center for Neutron Research for their assistance and helpful discussions. The QENS measurements were carried out at the NIST Center for Cold Neutron Research, which is supported in part by the National Science Foundation under Agreement No. DMR-0086210. Certain trade or names and company products are identified to adequatly specify the experimental procedure. In no case does such identification imply recommendation or endorsement by the National Institute of Standards and Technology, nor does it imply that the products are necessarily best for the purpose.

References

1. Ellis RJ, Minton AP. Nature. 2003; 425:27. [PubMed: 12955122]
2. Pielak GJ. Proc Natl Acad Sci USA. 2005; 102:5901. [PubMed: 15840719]
3. Ball P. Chem Rev. 2008; 108:74. [PubMed: 18095715]
4. de A A Soler-Illia GJ, Sanchez C, Lebeau B, Patarin J. Chem Rev. 2002; 102:4093. [PubMed: 12428985]
5. Ying JY, Mehnert CP, Wong MS. Angew Chem Int Ed. 1999; 38:56.
6. Vallet- Regí M, Balas F, Arcos D. Angew Chem Int Ed. 2007; 46:7548.
7. Zanotti JM, Bellissent-Funel MC, Chen SH. Phys Rev E. 1999; 59:3084.
8. Schreiber A, Ketelsen I, Findenegg GH. Phys Chem Chem Phys. 2001; 3:1185.
9. Morishige K, Kawano KJ. Chem Phys. 1999; 110:4867.
10. Shirono K, Daiguji HJ. J Phys Chem C. 2007; 111:7938.
11. Rovere M, Gallo P. Eur Phys J E. 2003; 12:77. [PubMed: 15007683]
12. Gallo P, Rapinesi M, Rovere M. J Chem Phys. 2002; 117:369.
13. Gallo P, Rovere M, Spohr E. J Chem Phys. 2000; 113:11324.
14. Bellissent-Funel MC. Eur Phys J E. 2003; 12:83. [PubMed: 15007684]
15. Takahara S, Sumiyama N, Kittaka S, Yamaguchi T, Bellissent-Funel MC. J Phys Chem B. 2005; 109:11231. [PubMed: 16852371]
16. Liu L, Chen SH, Faraone A, Yen CW, Mou CY, Kolesnikov AI, Mamontov E, Leao J. J Phys: Condens Matter. 2006; 18:S2261.
17. Takamuku T, Yamagami M, Wakita H, Masuda Y, Yamaguchi T. J Phys Chem B. 1997; 101:5730.
18. Hwang DW, Chu CC, Sinha AK, Hwang LP. J Chem Phys. 2007; 126:44702.
19. Guégan R, Morineau D, Alba-Simionesco C. Chem Phys. 2005; 317:236.
20. Brodka A, Zerda ZW. J Chem Phys. 1996; 104:6319.
21. Aoyama N, Yoshihara T, Furukawa SI, Nitta T, Takahashi H, Nakano M. Fluid Phase Eq. 2007; 257:212.
22. Furukawa SI, Nishiumi T, Aoyama N, Nitta T, Nakano M. J Chem Eng Jap. 2005; 38:999.
23. Hellweg T, Schemmel S, Rother G, Brûlet A, Eckerlebe H, Findenegg GH. Eur Phys J E. 2003; 12:s1. [PubMed: 15011003]
24. Crowe JH, Carpenter JF, Crowe LM. Annu Rev Physiol. 1998; 60:73. [PubMed: 9558455]
25. Ciesla U, Schüth F. Micropor Mesopor Mater. 1999; 27:131.
26. Selvam P, Bhatia SK, Sonwane CG. Ind Eng Chem Res. 2001; 40:3227.
27. Lerbret A, Lelong G, Mason PE, Saboungi ML, Brady JW. Food Biophys. 2010 accepted.

28. Lelong G, Bhattacharyya S, Kline S, Cacciaguerra T, Gonzalez MA, Saboungi ML. J Phys Chem C. 2008; 112:10674.
29. Copley JR, Cook JC. Chem Phys. 2003; 292:477.
30. Meyer A, Dimeo RM, Gehring PM, Neumann DA. Rev Sci Instrum. 2003; 74:2762.
31. The IDL-based DAVE suite of programs was used to derive the scattering functions S(Q,E) (http://www.ncnr.nist.gov/dave/)
32. Franks F. Pure Appl Chem. 1987; 59:1189.
33. Brooks BR, Bruccoleri RE, Olafson BD, States DJ, Swaminathan S, Karplus M. J Comput Chem. 1983; 4:187.
34. Ryckaert JP, Ciccotti G, Berendsen HJC. J Comput Phys. 1977; 23:327.
35. Hockney RW. Methods Comput Phys. 1970; 9:126.
36. Steinbach PJ, Brooks BR. J Comput Chem. 1994; 15:667.
37. Brooks CL III, Pettit BM, Karplus M. J Chem Phys. 1985; 83:5897.
38. Kuttel M, Brady JW, Naidoo KJ. J Comput Chem. 2002; 23:1236. [PubMed: 12210149]
39. Berendsen HJC, Grigera JR, Straatsma TP. J Phys Chem. 1987; 91:6269.
40. Ziemys A, Ferrari M, Cavasotto CN. J Nanosci Nanotechnol. 2009; 9:6349. [PubMed: 19908533]
41. Ziemys A, Grattoni A, Fine D, Hussain F, Ferrari M. J Phys Chem B. 2010; 114:11117. [PubMed: 20738139]
42. Rovere M, Ricci MA, Vellati D, Bruni F. J Chem Phys. 1998; 108:9859.
43. Brovchenko I, Paschek D, Geiger A. J Chem Phys. 2000; 113:5026.
44. Brodka A, Zerda ZW. J Chem Phys. 1991; 95:3710.
45. Timasheff SN. Biochem. 2002; 41:13473. [PubMed: 12427007]
46. Shukla D, Shinde C, Trout BL. J Phys Chem B. 2009; 113:12546. [PubMed: 19697945]
47. Geerke DP, van Gunsteren WF, Hünenberger PH. Mol Sim. 2010; 36:708.
48. Errington JR, Debenedetti PG. Nature. 2001; 409:318. [PubMed: 11201735]
49. Branca C, Magazù S, Maisano G, Migliardo P. J Chem Phys. 1999; 111:281.Paolantoni M, Comez L, Fioretto D, Gallina ME, Morresi A, Sassi P, Scarponi F. J Raman Spectrosc. 2008; 39:238.
50. Lelong G, Price DL, Douy A, Kline S, Brady JW, Saboungi ML. J Chem Phys. 2005; 122:164504. [PubMed: 15945690]
51. Lelong G, Price DL, Brady JW, Saboungi ML. J Chem Phys. 2007; 127:65102.
52. Gladden JK, Dole M. J Am Chem Soc. 1953; 75:3900.
53. Xia Y, Dosseh G, Morineau D, Alba-Simionesco C. J Phys Chem B. 2006; 110:19735–19744. [PubMed: 17004844] Levchenko AA, Jain P, Trofymluk O, Yu P, Navrotsky A, Sen S. J Phys Chem B. 2010; 114:3070–3074. [PubMed: 20136110]
54. Lelong G, Howells WS, Brady JW, Talon C, Price DL, Saboungi ML. J Phys Chem B. 2009; 113:13079. [PubMed: 19739660]
55. Takahara S, Sumiyama N, Kittaka S, Yamaguchi T, Bellissent-Funel MC. J Phys Chem B. 2005; 109:11231. [PubMed: 16852371]
56. Spohr E, Hartnig C, Gallo P, Rovere M. J Mol Liq. 1999; 80:165.
57. Rampp M, Buttersack C, Lüdemann HD. Carbohydr Res. 2000; 328:561. [PubMed: 11093712]
58. Talón C, Smith LJ, Brady JW, Lewis BA, Copley JRD, Price DL, Saboungi ML. J Phys Chem B. 2004; 108:5120.
59. Mahoney MW, Jorgensen WL. J Chem Phys. 2001; 114:363.
60. Mark P, Nilsson L. J Phys Chem A. 2001; 105:9954.
61. Mills R. J Phys Chem. 1973; 77:685.
62. Gillen KT, Douglass DC, Hoch MJR. J Chem Phys. 1972; 57:5117.

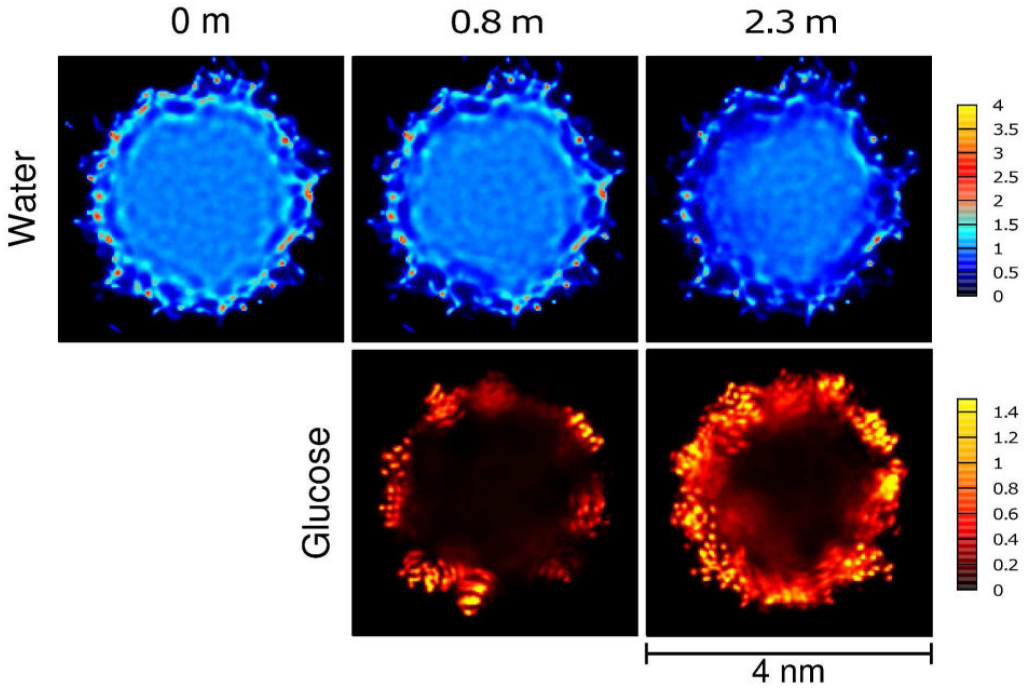

Fig. 1.

Average local XY densities ρ_{XY} of water (upper panel) and glucose (bottom panel) in the confined pure water (left) from [Ref. 27], 0.8 m (middle) and 2.3 m (right) glucose solutions.

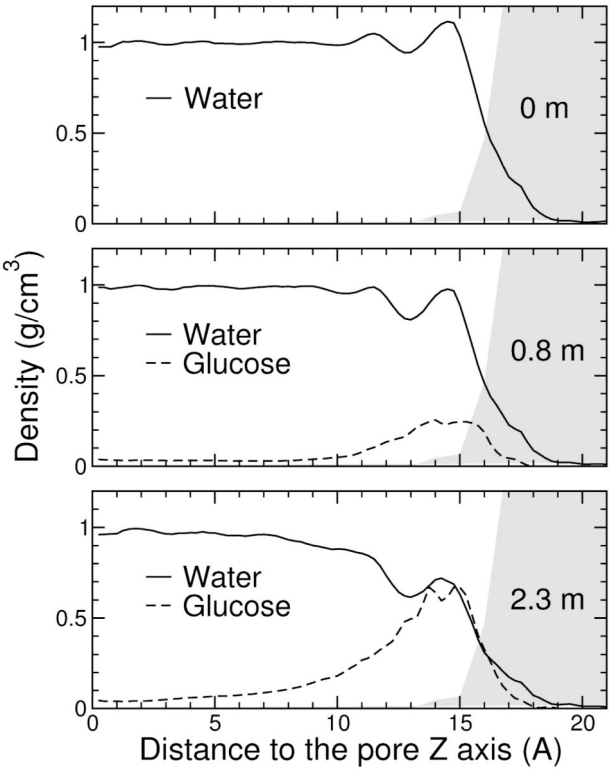

Fig. 2.

Water and glucose density profiles in the different studied confined solutions. The density profile of the silica matrix is also partly shown and shaded in grey to indicate the location of the pore surface.

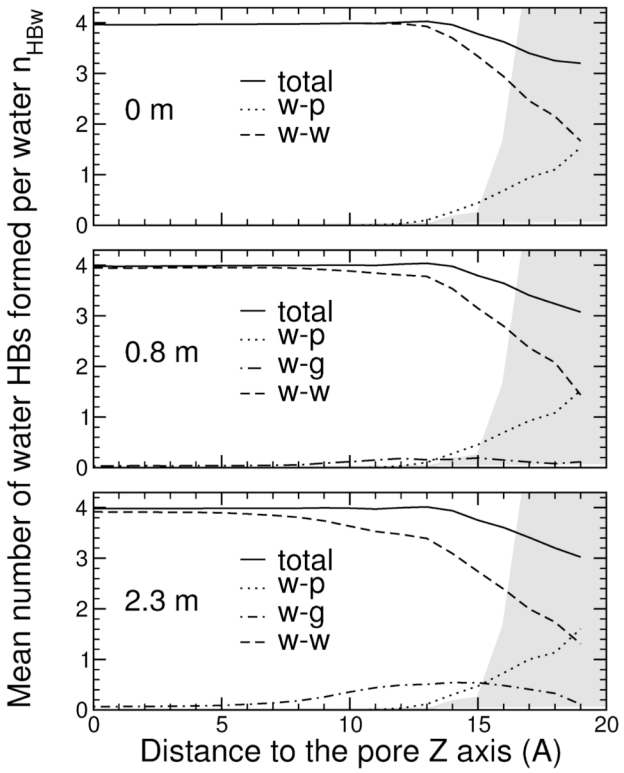

Fig. 3.

Mean number of HBs that a water molecule forms with other water (w-w) or glucose (w-g) molecules, or with the silica pore (w-p) as a function of its distance from the pore Z axis. The density profile of the silica matrix (plain gray shading) is shown to locate the pore surface.

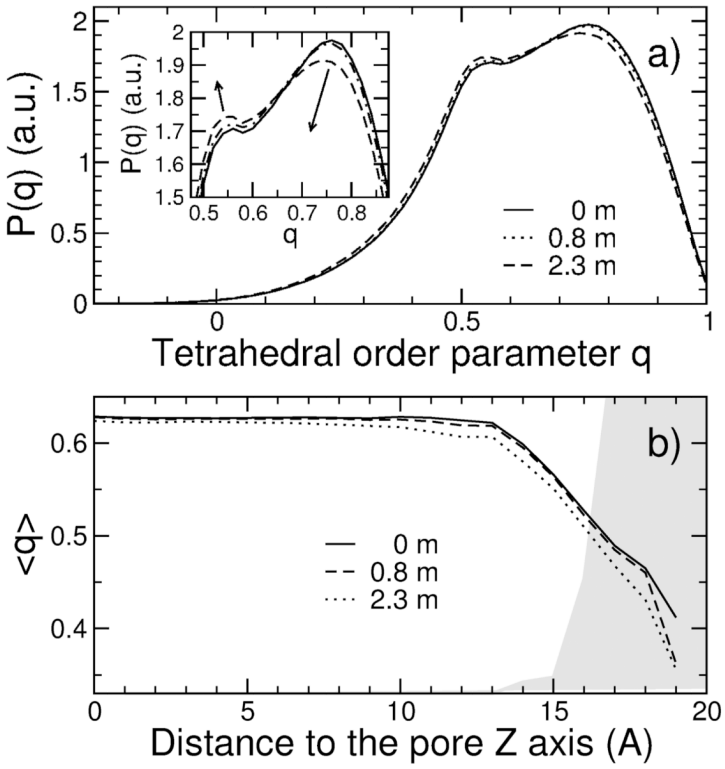

Fig. 4.

(a) Distribution functions of the orientational order parameter of water molecules in the $r <$ 12 Å region of the pore for the glucose solutions studied. The inset underlines the effect of glucose on the distribution of q, which is analogous to a slight temperature increase. (b) Radial evolution of the averaged water orientational order parameter for the glucose solutions studied. The density profile of the silica matrix (plain gray shading) is shown to locate the pore surface.

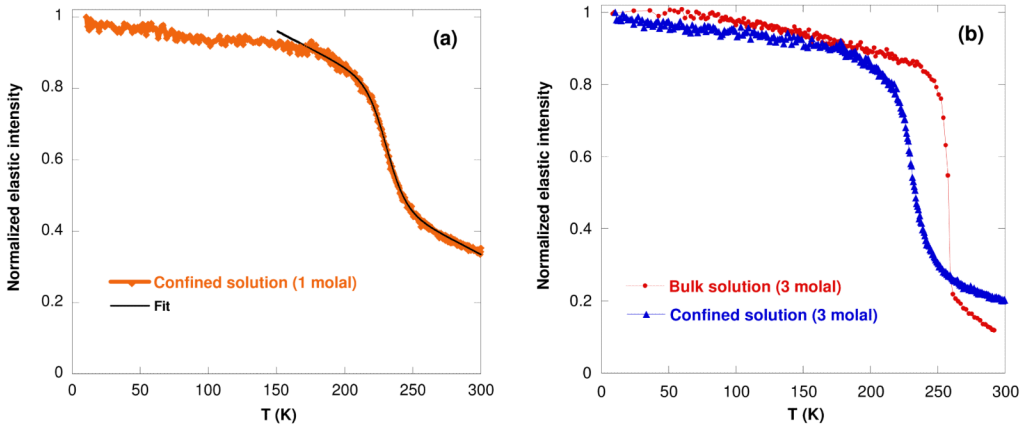

Fig. 5.

Elastic intensity as a function of the temperature *T* for (a) the 1 m confined glucose solution, and (b) the 3 m bulk and confined glucose solutions. Only the heating scans are shown here. The different background intensities observed at 300 K stem from a difference in the sample amount exposed to the neutron beam, and an increase of the coherent signal when adding sugar to water.

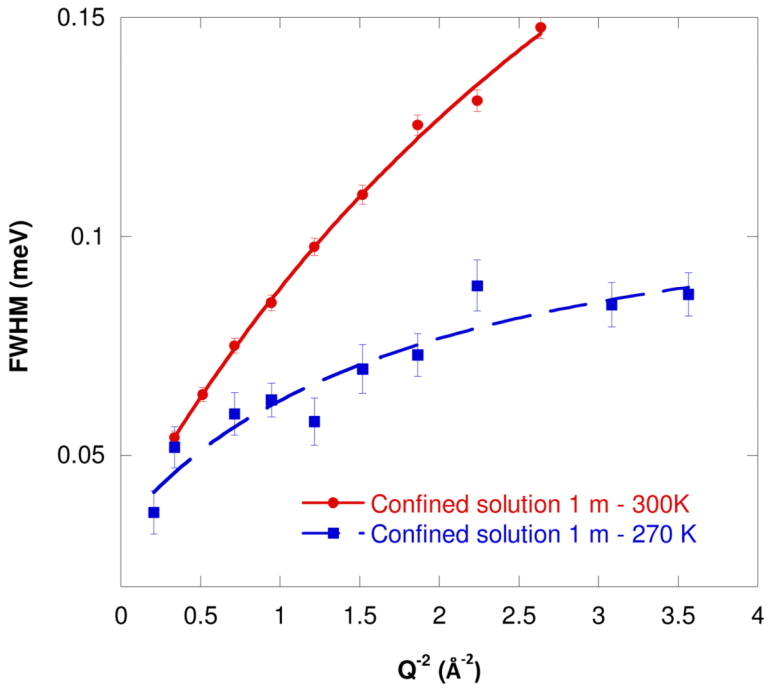

Fig. 6.

Full width at half maximum (FWHM) of the narrower Lorentzian fitted to the DCS QENS spectra vs. Q^2 for the confined glucose solution at 300 K (red) and 270 K (blue). The lines represent least-squares fits described in the text.

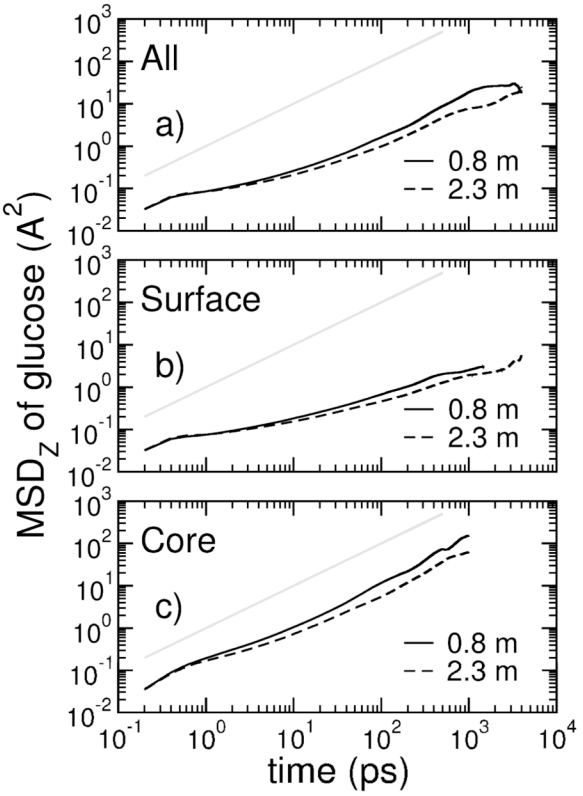

Fig. 7.

Mean-square displacement along the Z axis (MSD_Z) of the center of mass of glucose molecules in the whole pore (a) or in distinct parts of the pore: (b) in the surface ($r > 10$ Å) and (c) in the core ($r \leq 10$ Å) regions. Only the first part of the curves in the b and c figures are shown, because statistical errors arising from the computation of local MSDs are large at longer times. Grey lines with a unity slope are plotted to indicate a linear diffusion regime.

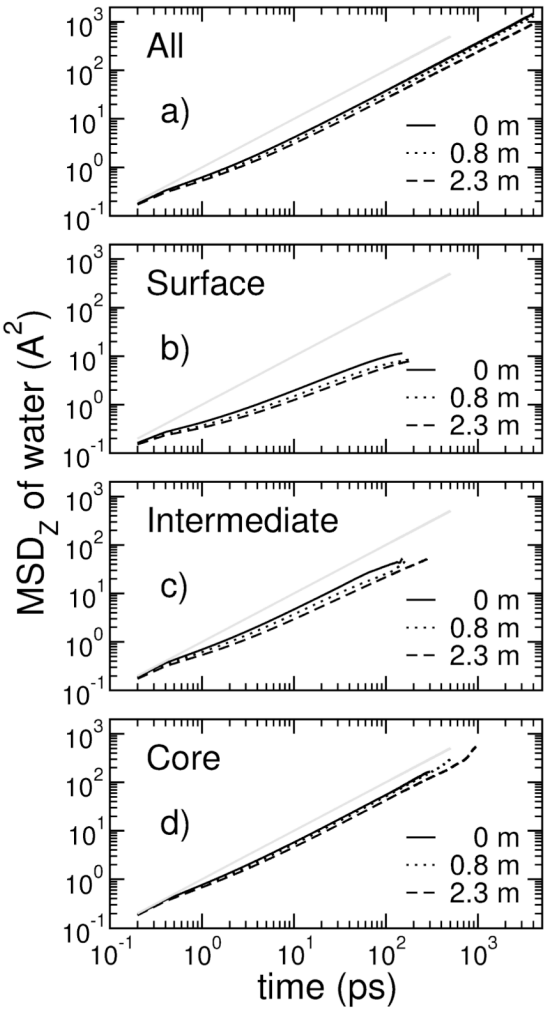

Fig. 8.

Mean-square displacement along the Z axis (MSD_Z) of the center of mass of water molecules in the whole pore (a) or in distinct parts of the pore: (b) in the surface ($r > 13$ Å), (c) in the intermediate ($9.2 < r \leq 13$ Å) and (d) in the core ($r \leq 9.2$ Å) regions. Only the first part of the curves in the b, c and d figures are shown, because statistical errors arising from the computation of local MSDs are large at longer times.

Table 1

Statistics of solution-pore HBs. W, G, and P stand for water, glucose, and pore, respectively

Concentration	W-P	G-P	W-P + G-P
0 m	322	-	322
0.8 m	289	35	324
2.3 m	229	77	306

Table 2

Physical constants calculated from the fits to FWHM as a function of Q^2 and compared with others experimental values found in the literature.[50]

	Confinement	Temp.	Instrument	$D_{glucose}$ ($\times 10^{-5}$ cm^{2}s^{-1})	l (Å)
This study (1 m)	MCM-41 (3.2 nm)	300K	DCS	0.5 ± 0.1	1.1 ± 0.4
		270K	DCS	0.3 ± 0.2	1.8 ± 0.7
		230K	HFBS	0.10 ± 0.03	4.7 ± 0.6
Lelong *et al.*[50] (1 m)	Aqueous silica gel (18 nm)	300K	DCS	0.74 ± 0.08	1.3 ± 0.1

Table 3

Translational diffusion coefficients along the pore Z axis D_Z of glucose molecules in the core region of the pore ($r \leq 10$ Å) for the two confined glucose solutions. The diffusion coefficients D of glucose molecules extrapolated from those computed in the simulated 1 m and 3 m bulk glucose solutions in [ref. 54] are also given for comparison.

Concentration	Confined D_Z (10^{-5} cm^2s^{-1}) (Core région)	Bulk D (10^{-5} cm^2s^{-1})
0.8 m	0.5	0.3
2.3 m	0.3	0.2

Table 4

Translational diffusion coefficients along the pore Z-axis D_Z of all water molecules or of only water molecules in the core region of the pore ($r \leq 9.2$ Å) for the different confined glucose solutions. The diffusion coefficients D of water molecules extrapolated from those computed in the simulated 1 and 3 m solutions in ref. 54 are also given for comparison.

Concentration (m)	Confined D_Z (10^{-5}cm^2/s)		Bulk D (10^{-5}cm^2/s)
	All water	Core region	
0	1.8	2.7	2.5
0.8	1.6	2.6	1.9
2.3	1.2	2.1	1.4